



Ultrafast singlet and triplet dynamics in microcrystalline pentacene films

Henning Marciniak,¹ Igor Pugliesi,² Bert Nickel,³ and Stefan Lochbrunner¹

¹*Institut für Physik, Universität Rostock, Universitätsplatz 3, 18051 Rostock, Germany*

²*Department of Physics, Lehrstuhl für BioMolekulare Optik, Ludwig-Maximilians-Universität, Oettingenstr. 67, 80538 München, Germany*

³*Department of Physics and CeNS, Ludwig-Maximilians-Universität, Geschwister-Scholl-Platz 1, 80539 München, Germany*

(Received 24 April 2009; published 16 June 2009)

The exciton dynamics of microcrystalline pentacene films is investigated by femtosecond pump-probe experiments. Measurements are performed with ultrashort laser pulses applied at normal incidence and at an angle of incidence of 65° to disentangle singlet and triplet contributions by exploiting the different orientations of the molecular transition dipoles. The results indicate that the initial 70 fs fast relaxation step transforms the optically excited excitons in a reasonable mobile species with strongly reduced radiative transition strength. Fission into triplet excitons takes place on the picosecond time scale as a secondary, thermally activated process and with a small total yield of approximately 2%. Evidence is provided that the dominant species are singlet excitons with excimer character. To the subsequent dynamics contribute diffusion driven exciton-exciton annihilation and trapping of singlet and triplet excitons. Values for diffusion constants and trap densities are extracted by modeling the measurements with rate equations which include singlet and triplet dynamics.

DOI: [10.1103/PhysRevB.79.235318](https://doi.org/10.1103/PhysRevB.79.235318)

PACS number(s): 71.35.Aa, 72.80.Le, 73.61.Ph, 78.66.Qn

I. INTRODUCTION

Organic materials have attracted strong scientific attention with respect to potential applications in photonics and electronics.^{1,2} In particular polyacenes have been intensively studied to understand the properties of organic crystals. Singlet and triplet excitons in naphthalene, anthracene, and tetracene crystals and the interaction between them are well characterized³ and the analysis of their properties has achieved a microscopic level.^{4,5} In crystalline pentacene films the situation is much less clear and the photoinduced dynamics and the relevant relaxation pathways are subjects of current research.⁶ Steady-state experiments are suitable to investigate the electronic excitations which are directly optical accessible^{7,8} but have not revealed much insight into the subsequent processes since the fluorescence of crystalline pentacene is extremely weak and does not provide the necessary information.^{9,10}

Meanwhile a number of time-resolved studies have been carried out. Terahertz experiments find free-charge carriers after excitation at 400 nm which are trapped within a few picoseconds.¹¹ Similar studies with excitation in the visible spectral range again observe signatures of free charge carriers.¹² However, the signal strength points in this case to a yield for charge generation in the order of 1%. Time-resolved photoconductivity experiments on films of substituted pentacene confirm the appearance of free charge carriers but the yield again indicates that they are probably not the dominant species.¹³ Absorption studies on the femtosecond time scale point to the relevance of singlet and triplet excitons. For pentacene films a very fast dynamics with a time constant of about 70 fs was found.^{9,14} This dynamics was interpreted as fission of the primarily excited singlet excitons into two triplet excitons.^{9,15} In larger polyacenes the energy of the triplet state is about half of the energy of the first electronically excited singlet state. In crystals singlet excitons can then split into two triplet excitons under conser-

vation of the total spin. Exciton fission was previously observed in tetracene as a thermally activated process^{16,17} where the energy of the lowest-excited singlet state is about 0.2 eV lower than twice the energy of the lowest triplet state. In pentacene the energy of the lowest-excited singlet state in the ground-state geometry is 1.83 eV (Refs. 7 and 18) and thereby more than twice the triplet energy of 0.86 eV.¹⁹ The fission might then be barrier free and extrapolating from the situation in tetracene to pentacene results in a theoretical time constant of 85 fs which would be in very good agreement with the experiments.⁹ However, the assignment of the transient absorption bands to triplet excitons does not reflect the electronic structure of the monomer.¹⁴ Little is known also on the subsequent dynamics of the excitons in pentacene and the dominant processes are not yet characterized. Recently, we observed signatures for annihilation processes in pentacene.¹⁴ But only a crude analysis of the dynamics could be provided at that time.

In this paper we present a transient absorption study on microcrystalline pentacene films with a time resolution of 30 fs and use the orientation of the singlet and triplet transition dipoles to disentangle the triplet from the singlet dynamics. Evidence is provided that the ultrafast initial relaxation step results again in a singlet species and triplet excitons are formed in a second step on a picosecond time scale and only with a low yield in the order of 2%. A model is developed which describes the annihilation and relaxation dynamics and takes the interplay between singlet and triplet excitons into account.

II. EXPERIMENT

Samples of thin microcrystalline films are prepared by vacuum deposition of pentacene on a transparent polymer substrate [thermoplastic olefin polymer of amorphous structure (TOPAS)]. The film consists of closely packed crystal-

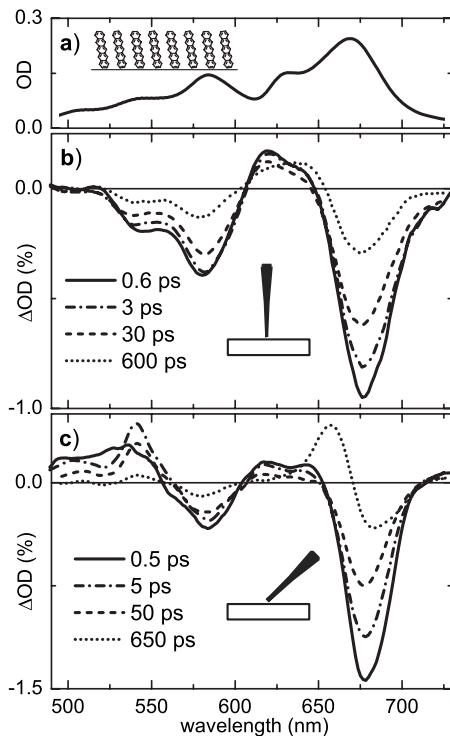


FIG. 1. (a) Steady-state absorption spectrum of a microcrystalline pentacene film, (b) transient absorption spectra at different delay times after photoexcitation at 670 nm measured with laser beams normal to the substrate, and (c) transient spectra with beams at an angle of incidence of 65° .

line grains with a diameter of about $1 \mu\text{m}$ and a height of roughly 30 monolayers.²⁰ The samples are kept under nitrogen for storage and during the optical experiments. In the pump-probe measurements the samples are excited by 30-fs-long pulses with a center wavelength of 670 nm which are generated by a noncollinearly phase-matched optical parametric amplifier (NOPA) (Ref. 21) pumped by a 1 kHz regenerative Ti:sapphire amplifier system (CPA 2001; Clark MXR). The absorption changes are probed over the whole visible spectral range with a white light continuum. Pump and probe beams are overlapped and focused to a spot of $260 \mu\text{m}$ in diameter at the sample which is oriented normal to the beams or with an angle of incidence of 65° . The recollimated probe beam is dispersed with a prism after the sample²² and the transmitted energy is spectrally resolved measured with a photodiode behind a slit. The pump polarization is adjusted parallel to the probe beam with an achromatic $\lambda/2$ -wave plate.

III. RESULTS AND DISCUSSION

A. Evolution of the transient absorption

The steady-state absorption spectrum of the pentacene films [see Fig. 1(a)] is identical to earlier published ones.^{8,12} The oscillator strength of the bands originates from the molecular $S_1 \leftarrow S_0$ transition. In the crystalline phase the lowest absorption band is redshifted compared to the monomer absorption and exhibits additional structure due to Davydov splitting.^{3,12}

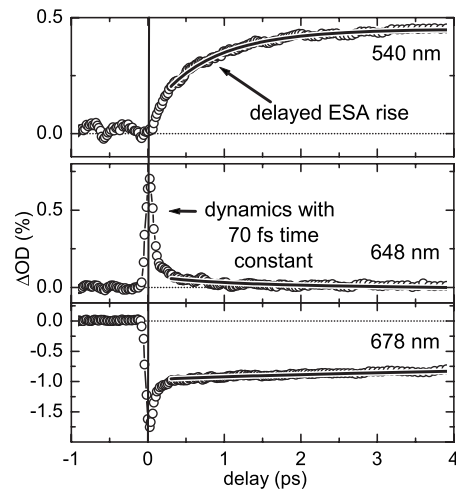


FIG. 2. Time traces measured with tilted angle of incidence (65°) of the pump and probe pulses at different probe wavelengths. The solid lines represent simulations with a model that describes the exciton dynamics on the ps time scale subsequent to the initial ultrafast relaxation process (for details see text).

Transient spectra were measured with an angle of incidence for the laser pulses of 0° and of 65° at various delay times after photoexcitation in the lowest absorption band at 670 nm. The transient spectra recorded at normal incidence [see Fig. 1(b)] are in good agreement with those reported in Ref. 23. They show a strong ground-state bleach and excited-state absorption (ESA) which is most evident in the region between 600 and 650 nm. The bleach recovers to a large extent within several hundred picoseconds. There are no indications for stimulated emission (SE). This is in agreement with the fact that crystalline pentacene exhibits only very weak fluorescence.^{9,10} The transient spectra measured with an angle of incidence of 65° show a very similar behavior as spectra at normal incidence [see Fig. 1(c)]. However, around 540 nm an additional absorption band is observed which appears with a small delay.

Figure 2 shows kinetic traces measured at 540, 648, and 678 nm at tilted incidence of the laser pulses. The presented probe wavelengths correspond to the two ESA bands and the spectral region where the bleach is dominant. The traces at 648 and 678 nm exhibit an ultrafast component with a time constant of about 70 fs. This component was already observed previously^{9,14} and indicates an ultrafast relaxation process of the optically excited excitons. Contrary to that, the dynamics of the absorption at 540 nm shows a much slower rise on a time scale of about 1 ps. The subsequent evolution of the transient spectra is dominated by a general decay of the bleach and absorption signatures. In addition some spectral reshaping is observed in the region of the ESA. The kinetic traces measured at various wavelengths show a rather complex, strongly nonexponential behavior and depend on the excitation density (see Figs. 4, 5, and 7). In the next two sections a model is developed to explain the evolution of the transient spectra.

B. Singlet versus triplet dynamics

In the following we discuss the ultrafast dynamics during the first few picoseconds. The initial 70 fs component (see

Fig. 2) was observed previously by others⁹ and by us.¹⁴ Originally, it was assigned to the fission of the primarily generated singlet excitons into, respectively, two triplet excitons due to the arguments given in the introduction.^{9,15} Accordingly, the ESA band observed at normal incidence around 630 nm was attributed to triplet excitons. In solution, the triplet absorption exhibits an intense band at 505 nm which is 1 order of magnitude stronger than that of the $S_1 \leftarrow S_0$ transition.²⁴ Compared to that, the ESA signature in the transient spectra is relatively weak. At first glance this seems to be an indication for a very small triplet population. However, the transition dipole of the triplet state is oriented along the long axis of the molecules.^{24,25} Since the pentacene molecules are standing almost upright on the substrate surface,²⁶ the dipole is perpendicular to the electric fields of the laser pulses in the case of normal incidence and can hardly interact with them. Hence it is unlikely that the signature between 600 and 650 nm is a result of triplet state absorption. Tilting the angle of incidence of the laser pulses should give rise to a strengthening of absorption signatures due to triplet excitons. Measurements with an angle of incidence of 65° [see Fig. 1(c)] show no increase in the ESA between 600 and 650 nm but a new ESA signature at 540 nm, which does not appear in the spectra measured at normal incidence. Consequently we assign this signature to the triplet excitons. However, the new band is also relatively weak indicating that the fission process has a low-quantum yield and does not play a dominant role in the overall dynamics.

Kinetic traces measured with an angle of incidence of 65° at the probe wavelengths 648 and 678 nm, which reflect the dynamics of the low-energy ESA band and the bleach, show very clearly the 70 fs component (see Fig. 2). The trace recorded at 540 nm corresponding to the triplet absorption lacks this feature and shows a much slower absorption rise on the picosecond time scale. The 70 fs relaxation of the optically excited excitons results obviously not in triplet excitons but in a different species. The triplets are formed in a second step and accordingly to the weak signal with a low yield.

The species formed by the first relaxation step has no or only a very weak radiative decay channel back to the electronic ground state since the transient spectra measured after 100 fs show no indication for stimulated emission. We suggest that the nature of this species might be best described as very similar to excimers.¹⁴ In this case two neighboring molecules form a bound dimer in the electronically excited state. To check the plausibility of this suggestion we performed time dependent DFT (TDDFT) (Ref. 27) calculations on the dimer consisting of two coplanar pentacene molecules. The calculations were carried out using the TURBOMOLE program package^{28,29} and employing the B3LYP functional and the Karlsruhe split valence basis set^{30,31} augmented with one polarization function. The ground-state geometry was optimized without symmetry constraints with a coplanar arrangement of the monomers. The resulting equilibrium structure conserved the coplanar form. The intramolecular bond lengths and bond angles of the cluster moieties are very similar to those found for an optimized pentacene monomer indicating that the aggregation does not affect significantly the monomer structure. The geometric parameters of the penta-

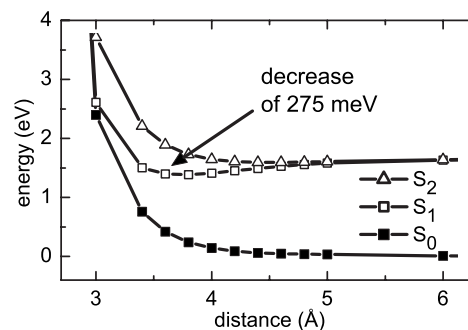


FIG. 3. *Ab initio* calculation (TDDFT) of the S_0 , S_1 , and S_2 energies of the pentacene dimer depending on the distance between two coplanar pentacene molecules.

cene monomers obtained from the dimer ground-state optimization were then used to calculate vertical energies at several intermonomer distances in the coplanar arrangement. For all calculated points the two lowest-lying excited states (S_1 and S_2) are linear combinations of the lowest locally excited states of the monomers and thus possess excitonic character.

Figure 3 shows the energies of the electronic ground state and the two lowest electronically excited singlet states of the dimer in dependence on the intermolecular distance. The minimum of the electronic ground state is at an intermolecular distance of about 6 Å while the minimum of the S_1 state is at a distance of 3.6 Å and 275 meV below the S_1 energy of the ground-state equilibrium point at 6 Å. It indicates that the formation of an excimer, e.g., a more tightly bound electronically excited dimer can lead to an energy decrease in the order of 0.3 eV. The energy of the S_1 state is then below twice the triplet energy and triplet fission is associated with a barrier. In this way the first relaxation step causes a strong decrease in the fission rate and the yield for triplet excitons is drastically reduced in agreement with the experiment. In the crystal structure the pentacene molecules are not coplanar but tilted with respect to each other. The excimer formation should then be associated with a slight rotation of two neighboring molecules in addition to a reduction in the distance to achieve a more parallel orientation and a better interaction of their electronic π systems. In a coplanar arrangement the $S_1 \leftarrow S_0$ transition is electric dipole forbidden.³ Accordingly, the formation of excimers would cause ultrafast emission quenching and can explain the absence of stimulated emission at later times and the low photoluminescence yield of crystalline pentacene.

Other possibilities for the nature of the species also have to be considered. It was suggested that charge-transfer excitons^{7,32,33} or free charge carriers^{23,34} are generated. The formation of excitons with strong charge-transfer character or the ultrafast dissociation into free charges can also explain the lack of emission. In both cases transient spectral signatures are expected which are related to the electric-dipole transitions of the molecular anion or cation. Both ions have absorption bands in the near infrared (NIR) and in the blue spectral region, the cation, e.g., at 425 nm.^{35,36} In the region 380–480 nm we find only a weak and completely flat absorption in the transient spectra (not shown) and no indication for

a cation band. This is in agreement with previous studies on the microsecond time scale, which found no indication for any cation absorption also in the NIR.¹⁵ Since pentacene ions show no absorption in the region 700–460 nm, it is also unlikely that they contribute to the transient absorption observed in this region. From these findings we conclude that free charges are not generated in a high yield and the character of the species generated by the primary relaxation step is not dominated by charge-transfer contributions. However, ionic absorption features might be hidden by the structureless ESA signal below 480 nm and a significant contribution of free charges below $\sim 10\%$ or a certain amount of charge transfer cannot be excluded. Accordingly, the nature of the emerging species is not completely established and demands further investigation. But for simplicity and because of its mobility, the species will be referred to as singlet excitons in the following.

The delayed rise of the triplet ESA observed at 540 nm can be modeled as a thermally activated process as it is shown below. This points to an energy barrier for the fission process and the energy of the state formed by the first relaxation step seems to be less than twice the energy of the triplet state in agreement with the arguments given above. The energy released by the primary relaxation process is initially distributed only over a few vibrational degrees of freedom and dissipates then into the crystal. This leads to an elevated local temperature directly after the first relaxation step which cools down to room temperature with time. This scenario results in the time-dependent triplet population $n_T(t)$ described by Eqs. (1)–(3) if an Arrhenius-type behavior for the fission rate is assumed,

$$n_T(t) = A(t) \int_0^t \exp\left(-\frac{E_{\text{barrier}}}{k_B T(t')}\right) dt', \quad (1)$$

$$A(t) = 2k_A n_S(t), \quad (2)$$

$$T(t) = \Delta T \exp\left(-\frac{t}{\tau_{\text{cooling}}}\right) + 300 \text{ K}. \quad (3)$$

The prefactor $A(t)$ takes into account that two triplets are formed per fission event. It includes the singlet population $n_S(t)$ which turns out to be time dependent (see below) and the barrier free rate of the fission process $k_A = (85 \text{ fs})^{-1}$ that is derived by extrapolation from the measured fission rate in tetracene.¹⁶ E_{barrier} denotes the energy barrier and $T(t)$ is the temperature which decays exponentially with the cooling time τ_{cooling} to 300 K. In the next section the time dependence of the singlet population $n_S(t)$ is discussed and modeled. It is taken into account to obtain a completely consistent picture. To model the data Eq. (1) is integrated simultaneously with Eqs. (6)–(10) which describe the complete dynamics after the first relaxation step (see Sec. III B). Since the 70 fs process is not included the simulation starts after the first 300 fs. Good agreement with the data is obtained if an energy barrier E_{barrier} of 0.3 eV, an initial temperature rise ΔT of 210 K, and a cooling time τ_{cooling} of 2.1 ps are chosen (Table I). The modeled triplet signal is shown as solid line in Fig. 2(a). Other combinations of values

TABLE I. Parameters resulting from modeling the measured data with Eqs. (6)–(10).

D_S	$5 \times 10^{-4} \text{ cm}^2/\text{s}$
k_{relax}	$(30 \text{ ps})^{-1}$
k_{long}	$(1200 \text{ ps})^{-1}$
$N_{\text{trap } S}$	$1.7 \times 10^{19} \text{ cm}^{-3}$
D_T	$13.5 \times 10^{-4} \text{ cm}^2/\text{s}$
$N_{\text{trap } T}$	$0.15 \times 10^{19} \text{ cm}^{-3}$
E_{barrier}	0.3 eV
ΔT	210 K
τ_{cooling}	2.1 ps

within a range of $\pm 30\%$ give similar good results. From the molecular energies of the singlet and triplet states and from the TDDFT calculations of the dimer an energy barrier of 0.1 eV would be estimated. The barrier in the model is in the same order of magnitude and the difference can easily result from neglecting crystal effects in the estimation. The temperature rise of 210 K corresponds to a distribution of the energy released by the excimer formation over 15 vibrational modes with low frequencies. This seems to be reasonable for a local distortion of the crystal structure. The cooling time of 2.1 ps is comparable to the time scale of intraband relaxation in pentacene, which was recently characterized by simulations.³⁷

C. Diffusion-controlled dynamics

In the picosecond regime the measured data exhibit complex dynamics that cannot be described by a simple exponential behavior (see Figs. 5 and 7). Furthermore the variation in the excitation energy reveals an excitation intensity dependence of the bleach recovery (see Fig. 4). This is an indication for exciton-exciton annihilation, which has been observed repeatedly in organic thin films at sufficient excitation intensities.^{38,39}

The annihilation process can roughly be described as follows.³ It is assumed that the excitons diffuse through the material by “hopping” between neighboring sites of the mo-

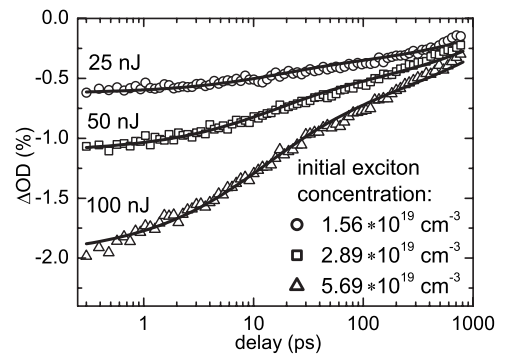


FIG. 4. Time traces measured at 685 nm with different excitation energies modeled with Eqs. (6)–(10) (solid lines). The initial exciton concentrations are obtained by the fitting procedure and scale correctly with the pump energies. For details see text.

molecular crystal. Whenever two excitons reach a critical distance to each other, which is assumed to be in the order of the lattice constant, they can interact and one of the participating molecules is excited into a higher electronic state S_n while one exciton relaxes to the ground state S_0 . It is usually assumed that the higher excited state decays almost immediately to the S_1 state by internal conversion and a single exciton remains.³⁸ The annihilation rate of the excitons depends on the average distance between them and on their concentration $n(t)$. This leads to a rate equation with a time-dependent rate,

$$\frac{dn(t)}{dt} = -\gamma(t)n(t)^2. \quad (4)$$

The expression for $\gamma(t)$ can be obtained from the approximate solution for the equivalent problem of coagulating particles⁴⁰

$$\gamma(t) = f8\pi D\bar{a} \left(1 + \frac{\bar{a}}{\sqrt{2\pi Dt}} \right). \quad (5)$$

D is the diffusion constant, \bar{a} is the average lattice constant, and f is a factor which is set to 1, if no exciton survives the annihilation event, or to $\frac{1}{2}$, if one exciton remains as in the case considered here.

Several models, which all include diffusion-controlled exciton-exciton annihilation as dominant process, were fitted to the measured data (see Fig. 5). To this end rate equations for the contributing species were formulated and numerically integrated. Parameters such as the diffusion constant and signal amplitudes were optimized in an iterative procedure using a Gauss-Newton algorithm.

The pure annihilation model shows poor agreement with the data (see dashed line in the upper graph of Fig. 5) and adding a single exponential decay for the natural exciton lifetime yields an unphysical negative time constant. The model was extended to account for traps in the imperfect lattice of the microcrystalline films, which can immobilize excitons (dotted lines in Fig. 5). This gives a good description of the dynamics at 685 nm, where the bleach is dominant. In addition, the excitation dependence of this dynamics is reproduced very well. This is shown for the final formulation of the model in Fig. 4. The initial exciton concentration was calculated for the highest excitation energy of 100 nJ (open triangles) while the other parameters are chosen consistently with the fit results of the data presented in Fig. 5. In the case of the two lower excitation energies solely the initial exciton concentrations were optimized. The model is in good agreement with the data and the resulting exciton concentrations (given in Fig. 4) scale nicely with the pump pulse energies. However, the data are insufficiently reproduced in the spectral region between 600 and 650 nm, where the dynamics is more complex due to spectral changes in the ESA. Therefore a relaxation process of the trapped excitons was added in a second step. With this model a consistent fitting of the complete data measured in all spectral regions is possible (solid lines in Fig. 5) and also the dependence on the excitation intensity is described correctly (see Fig. 4). Incorporating the thermally activated process of triplet exciton gen-

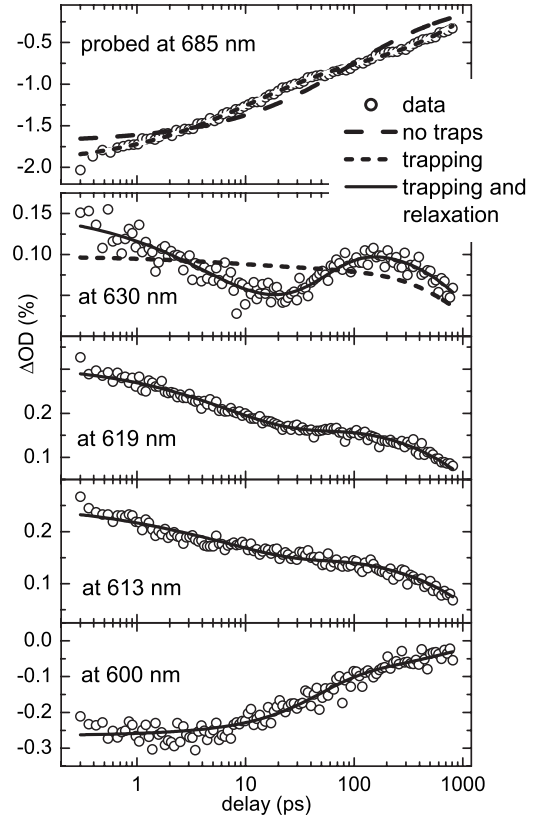


FIG. 5. Time traces at normal incidence of the laser pulses probed at 685 nm and at different wavelengths in the spectral region of the ESA. The dashed line in the most upper graph results from a fit with a model of pure exciton annihilation. The dotted lines in the two upper graphs denote a fit with a model additionally accounting for the immobilization of excitons at traps. The solid lines show a consistent fit of all measured time traces achieved with Eqs. (6)–(10). For details see text.

eration as well as the following triplet dynamics (see below) in the model does hardly affect the fit of the time traces measured at normal incidence but yields consistent fits for the time traces measured with tilted angle of incidence (see Fig. 7). A schematic picture of the contributing processes is shown in Fig. 6.

The resulting system of differential equations used for modeling the data reads,

$$\begin{aligned} \frac{dn_S(t)}{dt} = & -\frac{1}{2}8\pi D_S\bar{a} \left(1 + \frac{\bar{a}}{\sqrt{2\pi D_S t}} \right) n_S(t)^2 \\ & - 4\pi D_S\bar{a} \left(1 + \frac{\bar{a}}{\sqrt{\pi D_S t}} \right) n_S(t) \\ & \times [N_{\text{trap } S} - n_{\text{trap } S}(t) - n_{\text{traprel } S}(t)] - k_A \\ & \times \exp \left\{ -\frac{E_{\text{barrier}}}{k_B \left[\Delta T \exp \left(-\frac{t}{\tau_{\text{cooling}}} \right) + 300 \text{ K} \right]} \right\} n_S(t), \end{aligned} \quad (6)$$

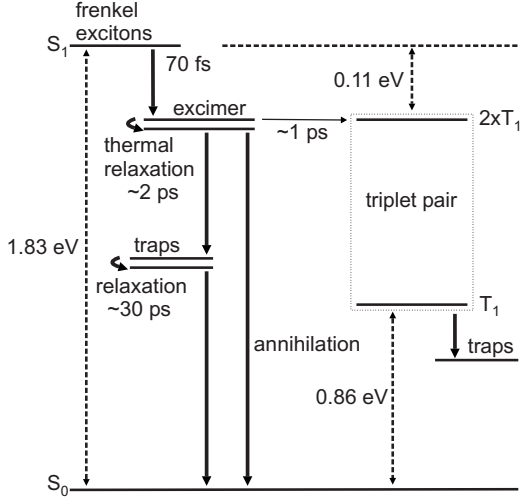


FIG. 6. Energy diagram and relaxation pathways.

$$\frac{dn_{\text{trap } S}(t)}{dt} = 4\pi D_S \bar{a} \left(1 + \frac{\bar{a}}{\sqrt{\pi D_S t}}\right) n_S(t) \times [N_{\text{trap } S} - n_{\text{trap } S}(t) - n_{\text{traprel } S}(t)] - k_{\text{relax}} n_{\text{trap } S}(t), \quad (7)$$

$$\frac{dn_{\text{traprel } S}(t)}{dt} = k_{\text{relax}} n_{\text{trap } S}(t) - k_{\text{long}} n_{\text{traprel } S}(t), \quad (8)$$

$$\frac{dn_T(t)}{dt} = 2k_A \exp\left[-\frac{E_{\text{barrier}}}{k_B \left[\Delta T \exp\left(-\frac{t}{\tau_{\text{cooling}}}\right) + 300 \text{ K}\right]}\right] n_S(t) - 4\pi D_T \bar{a} \left(1 + \frac{\bar{a}}{\sqrt{\pi D_T t}}\right) n_T(t) [N_{\text{trap } T} - n_{\text{trap } T}(t)], \quad (9)$$

$$\frac{dn_{\text{trap } T}(t)}{dt} = 4\pi D_T \bar{a} \left(1 + \frac{\bar{a}}{\sqrt{\pi D_T t}}\right) n_T(t) [N_{\text{trap } T} - n_{\text{trap } T}(t)]. \quad (10)$$

Here n_S , $N_{\text{trap } S}$, $n_{\text{trap } S}$, and $n_{\text{traprel } S}$ are the concentrations of the singlet excitons, the traps, the trapped singlet excitons, and the relaxed trapped singlet excitons. The concentrations of triplet excitons n_T , and as it is discussed below of traps $N_{\text{trap } T}$, which are active for triplet excitons and of trapped triplet excitons $n_{\text{trap } T}$ have also to be considered. D_S and D_T are the singlet and triplet diffusion constants. k_{relax} is the inverted relaxation time and k_{long} the decay rate of the relaxed trapped excitons to the ground state. The parameters k_A , E_{barrier} , ΔT , and τ_{cooling} are defined as described in Sec. III B. The lattice constant \bar{a} was set to 1 nm, which is approximately the geometrical average of the lattice constants.^{26,38} The initial singlet exciton density $n_S(0)$ was calculated from the excitation intensity and the optical density of the pentacene films at 670 nm. The values of the parameters resulting from the fit are given in Table I.

The time traces (see Fig. 7) and the transient spectra [see Fig. 1(c)] measured with tilted angle of incidence show that

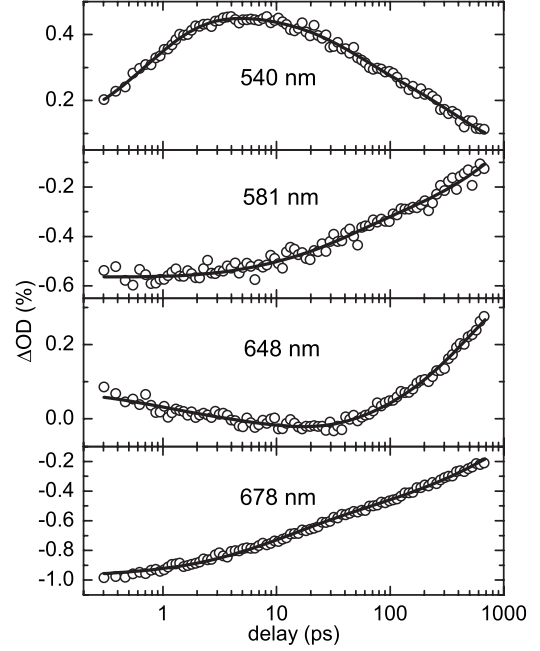


FIG. 7. Time traces measured with tilted angle of incidence of the laser pulses after photoexcitation at 670 nm at different probe wavelengths. The traces can be fitted with Eqs. (6)–(10) (black lines) with the same parameter values as for the measurements at normal incidence.

the band at 540 nm which is attributed to triplet excitons decays in about few hundred picoseconds while a second band at 655 nm rises. We model this dynamics as diffusion-controlled trapping at lattice defects while the intrinsic lifetime of triplet states should be on the μs time scale.²⁴ It is assumed that the trapped triplet excitons show a redshifted absorption and a lifetime much longer than the investigated time range. The assignment of the band at 655 nm to a triplet state is supported by the observation that it does not appear at normal incidence as expected from the orientation of the transition dipole along the long molecular axes (see Fig. 1). Triplet excitons in tetracene¹⁶ as well as in anthracene^{41,42} exhibit diffusive motion and exciton-exciton annihilation. In the present experiments there are no indications that triplet-triplet annihilation plays an important role. Probably the triplet yield and concentration are not large enough to lead to many annihilation events within the considered time window. From Fig. 1(c) it can be seen that the absorption of the trapped triplet excitons has about the same strength as the ground-state bleach. The assumption that the bleach results from population in the triplet state would be in contrast to the conception that the triplet excitons have a much larger absorption coefficient than the $S_1 \leftarrow S_0$ transition. Thus the relative strength of the bleach should result from long-lived singlet excitons. This is in agreement with the value of 1200 ps for the lifetime τ_{long} of the trapped and relaxed singlet excitons obtained by the fit.

Though the triplet dynamics show a significant contribution in the data measured with tilted angle of incidence of the laser pulses, the whole triplet yield is approximately 2%. This result of the fit is in agreement with the expected high absorption strength of the triplet excitons. It is also reflected

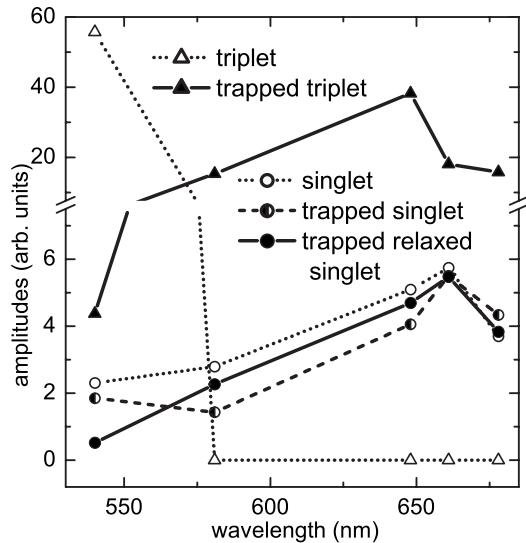


FIG. 8. Amplitude spectra resulting from the fit with Eqs. (6)–(10) of the time traces measured at tilted angle of incidence. The break in the ordinate accounts for the very different amplitudes of the singlet and triplet species.

by Fig. 8 which shows the fitted absorption amplitudes of the considered species for all modeled traces at tilted incidence. The absorption strength of the diffusing and the trapped triplet excitons is about 1 order of magnitude larger in the maximum than that of the singlet states as expected from the molecular absorption spectra. The amplitudes of the diffusing, trapped, and relaxed singlet excitons are similar indicating that the trapping and relaxation process result only in a slight shift and reshaping of the exciton absorption band. At normal incidence the differences are more pronounced (not shown).

In the following the obtained diffusion constants and trap concentrations are discussed. In Ref. 14 a preliminary model was presented which does not include the relaxation of the trapped excitons and the triplet contributions. For the singlet diffusion constant D_S the same value of $5 \times 10^{-4} \text{ cm}^2/\text{s}$ results in both models. Unfortunately, Ref. 14 contains a typo and D_S is erroneously given as $5 \times 10^4 \text{ cm}^2/\text{s}$. The diffusion constant can be compared to perylene crystals for which excimer excitons were observed and a diffusion constant of $5 \times 10^{-5} \text{ cm}^2/\text{s}$ was found.⁴³ The tenfold smaller constant might result from the higher binding energy of the perylene excimers of 0.4 eV which increases the barrier for hopping processes. The singlet diffusion constant in tetracene is about $4 \times 10^{-2} \text{ cm}^2/\text{s}$ (Ref. 44) and thereby almost 2 orders of magnitude larger than the one observed in pentacene. In tetracene the singlet excitons are common Frenkel excitons without excimer contribution.⁴⁵ Since the excimer formation is associated with a local deformation of the crystal structure, hopping barriers should be larger for excimer excitons than for common Frenkel excitons. Therefore, a reduced diffusion constant is expected for excimer excitons in agreement with the observation. The diffusion constant also provides evidence against the notion that free charges are the dominant species. In the latter case the holes, which have a mobility of more than $1 \text{ cm}^2/(\text{Vs})$ in crystalline pentacene,^{1,46} set a

lower limit for the diffusion constant of $2.5 \times 10^{-2} \text{ cm}^2/\text{s}$ via the Einstein relation $\mu = De_0/(k_B T)$.⁴⁷ This is 50 times higher than the observed value. The diffusion constant of the triplet excitons which results from modeling the observed dynamics is just in between the values reported for anthracene ($1.8 \times 10^{-4} \text{ cm}^2/\text{s}$) and tetracene ($4 \times 10^{-3} \text{ cm}^2/\text{s}$) (Refs. 3, 48, and 49) and fits to the general behavior of polyacene crystals. The obtained trap concentrations are quite high. However, there are several factors which in combination can account for the trap density. The microcrystals of the film have only a diameter of about $1 \mu\text{m}$ and are 50 nm thick.²⁰ They have a pyramidal shape with monolayer thick steps. The highly structured surface with its large area should provide a large number of defects. In addition, a high density of dislocation defects was observed in pentacene films by x-ray scattering.⁵⁰ It is also possible that excimer excitons are more sensitive to distortions of the crystal structure and localize more easily than other quasiparticles since their hopping probability is already comparable small.

IV. CONCLUSIONS

In conclusion, femtosecond transient absorption measurements on microcrystalline pentacene films reveal a detailed picture of their complex exciton dynamics. The singlet and triplet dynamics were disentangled with the help of the different orientations of the molecular transition dipoles by comparing experiments with the ultrashort laser pulses applied at normal incidence and at an angle of incidence of 65° . It is found that an initial 70 fs fast relaxation step transforms the optically excited excitons in a reasonable mobile species with strongly reduced radiative transition strength to the ground state. Fission into triplet excitons takes place on the picosecond time scale as a thermally activated process and with a small total yield of approximately 2%. Evidence is provided that the dominant species are singlet excitons with excimer character. However, the parallel generation of free charges with sufficiently low yield and charge-transfer contributions to the excitons cannot be excluded. The subsequent dynamics is dominated by diffusion-controlled processes. A model, which includes exciton-exciton annihilation, trapping of excitons, and a relaxation step of the trapped excitons, as well as the thermal activated fission into triplets, leads to a consistent description of all measured data. With this analysis absolute values for several important parameters such as diffusion constants and trap densities can be extracted. The results demonstrate that ultrafast spectroscopy reveals new insights in the microscopic dynamics and transport processes of molecular materials. The information will be helpful for the design of optoelectronic organic devices.

ACKNOWLEDGMENTS

We thank Florian Selmaier for help with the experiment, Jens Pflaum for providing purified pentacene, and Eberhard

Riedle for continuous support. The work was financially supported by the Deutsche Forschungsgemeinschaft within the collaborative research center under Grant No. SFB 652, the Cluster of Excellence: Munich-Centre for Advanced Photon-

ics and the Priority Program SPP 1121 as well as by CeNS. The Alexander von Humboldt Stiftung is gratefully acknowledged (I.P.) and the Leibniz-Rechenzentrum LRZ Munich for computing time and access to TURBOMOLE and GAUSSIAN.

- ¹C. D. Dimitrakopoulos, S. Purushothaman, J. Kyriassis, A. Callegari, and J. M. Shaw, *Science* **283**, 822 (1999).
- ²G. Malliaras and R. Friend, *Phys. Today* **58** (5), 53 (2005).
- ³M. Pope and C. E. Swenberg, *Electronic Processes in Organic Crystals and Polymers*, 2nd ed. (Oxford University Press, New York, 1999).
- ⁴S. H. Lim, T. G. Bjorklund, F. C. Spano, and C. J. Bardeen, *Phys. Rev. Lett.* **92**, 107402 (2004).
- ⁵T.-S. Ahn, A. M. Müller, R. O. Al-Kaysi, F. C. Spano, J. E. Norton, D. Beljonne, J.-L. Brédas, and C. J. Bardeen, *J. Chem. Phys.* **128**, 054505 (2008).
- ⁶M. Fiebig, C. Erlen, M. Göllner, P. Lugli, and B. Nickel, *Appl. Phys. A* **95**, 113 (2009).
- ⁷L. Sebastian, G. Weiser, and H. Bässler, *Chem. Phys.* **61**, 125 (1981).
- ⁸D. Faltermeier, B. Gompf, M. Dressel, A. K. Tripathi, and J. Pflaum, *Phys. Rev. B* **74**, 125416 (2006).
- ⁹C. Jundt, G. Klein, B. Sipp, J. Le Moigne, M. Joucla, and A. A. Villaeys, *Chem. Phys. Lett.* **241**, 84 (1995).
- ¹⁰E. J. Bowen, E. Mikiewicz, and F. W. Smith, *Proc. Phys. Soc. A* **62**, 26 (1949).
- ¹¹V. K. Thorsmølle, R. D. Averitt, X. Chi, D. J. Hilton, D. L. Smith, A. P. Ramirez, and A. J. Taylor, *Appl. Phys. Lett.* **84**, 891 (2004).
- ¹²O. Ostroverkhova, D. G. Cooke, S. Shcherbyna, R. F. Egerton, F. A. Hegmann, R. R. Tykwinski, and J. E. Anthony, *Phys. Rev. B* **71**, 035204 (2005).
- ¹³J. Day, S. Subramanian, J. E. Anthony, Z. Lu, R. J. Twieg, and O. Ostroverkhova, *J. Appl. Phys.* **103**, 123715 (2008).
- ¹⁴H. Marciniak, M. Fiebig, M. Huth, S. Schiefer, B. Nickel, F. Selmaier, and S. Lochbrunner, *Phys. Rev. Lett.* **99**, 176402 (2007).
- ¹⁵A. Saeki, S. Seki, and S. Tagawa, *J. Appl. Phys.* **100**, 023703 (2006).
- ¹⁶M. Pope, N. E. Geacintov, and F. Vogel, *Mol. Cryst. Liq. Cryst.* **6**, 83 (1969).
- ¹⁷R. P. Groff, P. Avakian, and R. E. Merrifield, *Phys. Rev. B* **1**, 815 (1970).
- ¹⁸K. O. Lee and T. T. Gan, *Chem. Phys. Lett.* **51**, 120 (1977).
- ¹⁹J. Burgos, M. Pope, C. E. Swenberg, and R. R. Alfano, *Phys. Status Solidi B* **83**, 249 (1977).
- ²⁰B. Nickel, M. Fiebig, S. Schiefer, M. Göllner, M. Huth, C. Erlen, and P. Lugli, *Phys. Status Solidi A* **205**, 526 (2008).
- ²¹E. Riedle, M. Beutter, S. Lochbrunner, J. Piel, S. Schenkl, S. Sporlein, and W. Zinth, *Appl. Phys. B: Lasers Opt.* **71**, 457 (2000).
- ²²M. Schlosser and S. Lochbrunner, *J. Phys. Chem. B* **110**, 6001 (2006).
- ²³V. K. Thorsmølle, R. D. Averitt, J. Demsar, D. L. Smith, S. Tretiak, R. L. Martin, X. Chi, B. K. Crone, A. P. Ramirez, and A. J. Taylor, *Phys. Rev. Lett.* **102**, 017401 (2009).
- ²⁴C. Hellner, L. Lindqvist, and P. C. Roberge, *J. Chem. Soc., Faraday Trans.* **68**, 1928 (1972).
- ²⁵M. Pabst and A. Köhn, *J. Chem. Phys.* **129**, 214101 (2008).
- ²⁶S. Schiefer, M. Huth, A. Dobrinevski, and B. Nickel, *J. Am. Chem. Soc.* **129**, 10316 (2007).
- ²⁷F. Furche and R. Ahlrichs, *J. Chem. Phys.* **117**, 7433 (2002).
- ²⁸O. Treutler and R. Ahlrichs, *J. Chem. Phys.* **102**, 346 (1995).
- ²⁹R. Ahlrichs, M. Bär, M. Häser, H. Horn, and C. Kölmel, *Chem. Phys. Lett.* **162**, 165 (1989).
- ³⁰A. Schäfer, H. Horn, and R. Ahlrichs, *J. Chem. Phys.* **97**, 2571 (1992).
- ³¹A. Schäfer, C. Huber, and R. Ahlrichs, *J. Chem. Phys.* **100**, 5829 (1994).
- ³²M. L. Tiago, J. E. Northrup, and S. G. Louie, *Phys. Rev. B* **67**, 115212 (2003).
- ³³Z. Wang, S. Mazumdar, and A. Shukla, *Phys. Rev. B* **78**, 235109 (2008).
- ³⁴O. Ostroverkhova, S. Shcherbyna, D. G. Cooke, R. F. Egerton, F. A. Hegmann, R. R. Tykwinski, S. R. Parkin, and J. E. Anthony, *J. Appl. Phys.* **98**, 033701 (2005).
- ³⁵D. Distler and G. Hohlneicher, *Ber. Bunsenges. Phys. Chem.* **74**, 960 (1970).
- ³⁶J. Szczepanski, C. Wehlburg, and M. Vala, *Chem. Phys. Lett.* **232**, 221 (1995).
- ³⁷M. Hultell and S. Stafström, *J. Lumin.* **128**, 2019 (2008).
- ³⁸E. Engel, K. Leo, and M. Hoffmann, *Chem. Phys.* **325**, 170 (2006).
- ³⁹M. A. Baldo, R. J. Holmes, and S. R. Forrest, *Phys. Rev. B* **66**, 035321 (2002).
- ⁴⁰M. v. Smoluchowski, *Z. Phys. Chem. (Leipzig)* **92**, 129 (1917).
- ⁴¹J. Jortner, S. A. Rice, and J. L. Katz, *J. Chem. Phys.* **42**, 309 (1965).
- ⁴²P. Avakian, V. Ern, R. E. Merrifield, and A. Suna, *Phys. Rev.* **165**, 974 (1968).
- ⁴³D. Fischer, G. Naundorf, and W. Klöpffer, *Z. Naturforsch. Teil A* **28**, 973 (1973).
- ⁴⁴A. J. Campillo, R. C. Hyer, S. L. Shapiro, and C. E. Swenberg, *Chem. Phys. Lett.* **48**, 495 (1977).
- ⁴⁵G. Vaubel and H. Baessler, *Mol. Cryst. Liq. Cryst.* **12**, 47 (1970).
- ⁴⁶O. D. Jurchescu, J. Baas, and T. T. M. Palstra, *Appl. Phys. Lett.* **84**, 3061 (2004).
- ⁴⁷S. M. Sze, *Physics of Semiconductor Devices* (John Wiley & Sons, New York, 1981), p. 28.
- ⁴⁸V. Ern, *Phys. Rev. Lett.* **22**, 343 (1969).
- ⁴⁹J. B. Aladekomo, S. Arnold, and M. Pope, *Phys. Status Solidi B* **80**, 333 (1977).
- ⁵⁰B. Nickel, R. Barabash, R. Ruiz, N. Koch, A. Kahn, L. C. Feldman, R. F. Haglund, and G. Scoles, *Phys. Rev. B* **70**, 125401 (2004).